

Influence of pulse-front curvature on vacuum acceleration by intense radially polarized laser beams

Spencer W. Jolly*

LIDYL, CEA, CNRS, Université Paris-Saclay, CEA Saclay, 91 191 Gif-sur-Yvette, France

(Dated: June 10, 2022)

We report with single particle simulations that pulse-front curvature, a commonly occurring spatio-temporal coupling equivalent to chromatic focusing, can have a significant influence in the on-axis longitudinal acceleration of electrons via high-power, tightly-focused radially polarized laser beams. This effect can be advantageous, and even more-so when combined with small values of temporal chirp. However, the effect can also be highly destructive when the magnitude and sign of the pulse-front curvature is not ideal, at very small magnitudes. This motivates the characterization and understanding of the driving laser pulses, and further study of similar low-order spatial-temporal couplings on such acceleration.

The direct acceleration of electrons to relativistic energies in vacuum is possible with a tightly focused, high power radially polarized laser beam (RPLB). The solution of the wave equation in focus produces a purely longitudinal field on axis, with a radial field towards the axis at points slightly off-axis [1]. This provides the motivation for using these beams to accelerate particles, either from rest or from modest energies, to relativistic energies [2]. We simulate the effects of spatio-temporal couplings (specifically longitudinal chromatism, or chromatic focusing) on such acceleration in two different scenarios.

The most general case of direct vacuum laser acceleration by an RPLB is that where a test particle begins from rest (or with a moderate initial energy) and an RPLB focuses and overtakes the particle. The longitudinal field in the focal region, when the laser power is large enough, imparts a net kinetic energy on the particle after overtaking. Detailed studies have been done showing especially that with optimization of both the initial position of the test particle and the carrier-offset phase (CEP), that the kinetic energy of the particle is always higher with decreasing duration and/or decreasing focused spot size [3]. These studies included particles beginning at rest and a large range of laser powers showing the suitability of the mechanism. Studies were also done including nonparaxial terms [4], off-axis fields [5] and even more complex interactions [6–8] showing that low energy-spread and collimation are indeed possible in a bunch of electrons with finite charge and size. Experimental results of this nature have been achieved in a low density neutral gas achieving 23 keV energies [9], and in a true vacuum, accelerating some electrons in a bunch from 40 keV up to a maximum of 52 keV [10].

Because this mechanism requires essentially for the particle to gain enough energy in a single cycle so as to not be fully decelerated in a subsequent cycle, there is a threshold power below which the particle will gain negligible energy. This has been shown to be related to the normalized beam intensity, and scales with w_0^4 [11]. Above this threshold the particle gains significant energy,

which is increasing with laser power. Well above the threshold the main limitation of such a scheme is that the accelerated particle inevitably slips out of the position of highest accelerating field since it is always travelling less than c , despite significant acceleration. The maximum electron energy from a transform limited pulse has been shown to scale with \sqrt{P} , with more tightly focused, shorter duration (or higher intensity) pulses approaching this limit [3].

The second scenario we approach is a restriction of the general case relating to electron acceleration from the interaction of an intense laser with a plasma mirror. In this complex nonlinear interaction the intense laser creates an overdense plasma at the surface of the dielectric, which then oscillates relativistically [12]. This mechanism can produce electrons, which were observed to be accelerated in vacuum from off-axis positions by the transverse field of the reflecting linearly polarized laser field [13]. There have been simulation studies showing that it is possible to have on-axis acceleration to high energies with the interaction of a radially polarized beam with such a plasma mirror [14]. This latter result is using the same basic physics as the more general case, with the most important contrast being that in this case the electrons begin with some energy (~ 0.2 MeV) and they are born from the plasma mirror oscillation within the focal volume at a set phase close to the optimum for direct acceleration [15]. Practically this means that the initial energy and position of the particle are fixed, where in the general scenario the position can be varied to optimize the acceleration, or only the electrons within a certain volume are accelerated well.

Beyond the standard use of a single Fourier-limited beam interacting with a single particle or bunch of particles, it may be possible to optimize the interaction with more complex or structured pulses, which we demonstrate in this work. A study was done in the general case using a beam composed of components of two colors with independent CEP [16]. The study showed a drastic increase in single particle accelerated energy with the same total laser power. This was due to the pulse beat-

ing within the Rayleigh range and the Gouy phase providing an advantageous situation for the particle to slip less out of the region of high accelerating field. Only certain differences in CEP between the different color pulses produced improved kinetic energies, corresponding to the case where the advantageous phase situation is created after the pulses focus, where the main acceleration occurs.

This concept of discrete multi-color fields in focus can be generalized to a specific continuous case, where the different colors of a single broadband (ultra-short) driving laser focus to different longitudinal positions. This is known as longitudinal (or axial) chromatism (LC), which in the near-field for a transform limited pulse takes the form as pulse-front curvature (PFC) or a radially varying group delay. In the farfield the pulse duration is increased according to the longitudinal separation of the spectral content. This is one of the well-known first-order spatio-temporal couplings [17]. This longitudinal chromatism can be induced simply by focusing via a singlet lens [18], by an afocal doublet made of special glasses [19], or via a diffractive lens [20] among other methods. The most commonly associated results from PFC is a decreased on-focus intensity.

In combination with temporal chirp this form of spatio-temporal/spatio-spectral coupling has been explored to control the velocity of the intensity peak of focused laser pulses, a 'Flying Focus' [19, 20]. However, the case explored here uses such small magnitudes of PFC and chirp such that the velocity of the intensity peak (and peak intensity) are not significantly affected, rather the effect on the phase within the Rayleigh range is also important. This is required for any effect on vacuum laser acceleration since both LC/PFC and chirp independently reduce the intensity in focus, and for such acceleration the electric field strength and thus intensity are key parameters. Effects of such an aberration on ultrashort pulses were observed on high-harmonic generation in gases [21]. We simulate the effect of PFC and chirp on vacuum laser acceleration in the general case, Scenario #1 (related to interaction with a low-density ambient gas) and the restricted case, Scenario #2 (related to interaction with a plasma mirror).

In all of the following simulations we use pulses that have Gaussian spatial and spectral profiles, with $w_0=4\mu\text{m}$ and $\tau_0=10\text{fs}$ characteristic widths respectively at a central wavelength of 800 nm ($\omega_0=2.36\times 10^{15}\text{rad/s}$). These both fit within the paraxial approximation. Although it has been shown that even in the case of $w_0=4\mu\text{m}$ ($\approx 5\lambda_0$) the results of acceleration off-axis including non-paraxial terms can be significantly different than the case without, the on-axis case is still valid [22]. Therefore the simulations presented here should be taken as valid only in the on-axis case. Additionally, since the manifestation of the nearfield PFC in focus depends on the focusing geometry, the corresponding near-field width

is chosen to be $w_i=4\text{cm}$ with a focal length of $f=63\text{cm}$.

The longitudinal field of the focused radial polarized field E_z is modeled with PFC α and group delay dispersion (GDD) ϕ_2 in the frequency space as in [19]. With $A(\omega) = \exp(-\delta\omega^2/\Delta\omega^2)$, $\Delta\omega = 2/\tau_0$, and $\delta\omega = (\omega - \omega_0)$ we have

$$\hat{E}_z(z, \omega) = \frac{1}{\Delta\omega} \sqrt{\frac{16P}{\pi\epsilon_0 c}} \frac{A(\omega)}{z_R \left(1 + \left(\frac{z-z_0(\omega)}{z_R}\right)^2\right)} e^{i\phi(z, \omega)} \quad (1)$$

$$\phi(z, \omega) = \Psi_0 + 2 \tan^{-1} \left(\frac{z - z_0(\omega)}{z_R} \right) - \frac{\phi_2 \delta\omega^2}{2} - \frac{\omega z}{c}, \quad (2)$$

with the Rayleigh length $z_R = 2cf^2/\omega_0 w_i^2$, the frequency dependent focus position due to the PFC/LC $z_0(\omega) = 2cf^2\alpha\delta\omega/\omega_0$, the CEP Ψ_0 , and the Fourier-limited pulse power P . In the time domain a positive α corresponds to a positive radial group delay. The acceleration of the electron is modeled by the relativistic Lorentz force equations

$$\frac{\partial \beta}{\partial t} = \frac{-q_e E_z(z, t)(1 - \beta^2)^{3/2}}{m_e c} \quad (3)$$

$$\frac{\partial z}{\partial t} = \beta c, \quad (4)$$

with q_e and m_e the electron charge and mass respectively, and $\beta = v/c$. We use a 5th-order Adams-Bashforth finite difference method to have improved accuracy with a fixed step size. The field $\hat{E}_z(z, \omega)$ is inverse Fourier transformed to t at each iteration to find the field at $z(t_i)$ and to calculate the next velocity and position. This step significantly increases the computation time compared to directly in the time domain. The simulations are run until the particle energy is no longer changing significantly, generally in the range of 10 ps for the power levels studied here. Results without any PFC or chirp were compared to those in the literature [3, 14] and agreed very well.

The two specific scenarios are detailed again technically in Fig. 1. In Scenario #1 the simulations start such that the laser pulse is far away from the test particle so as to have no influence, and propagates across the particle to impart a net kinetic energy. In every simulation — varying laser power, GDD, and PFC — we optimize the initial electron position $z(0)$ and CEP Ψ_0 for the maximum final kinetic energy, with the particles always beginning at rest. This emulates an experimental situation where the particles in a low-density gas would be distributed in space and the driving laser would have tunable CEP. In Scenario #2 the simulations start with the laser pulse already at best focus and the electron sitting at the first

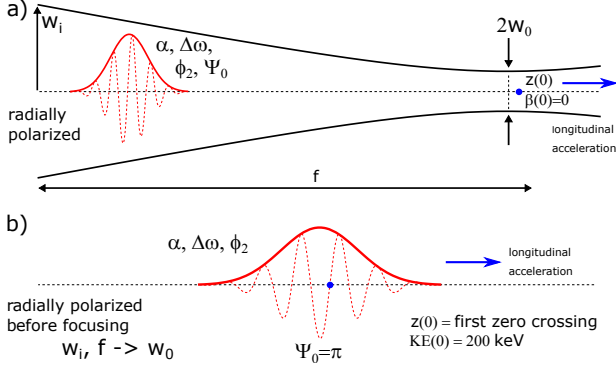


FIG. 1. Technical details of the two scenarios simulated here. These are the more general Scenario #1 (a) and the more restricted Scenario #2 (b). See the text for more details.

field zero in front of the field peak, with an initial kinetic energy of 200 keV. This second scenario requires no optimization at each set point due to the restrictions on the electron parameters, but would also require a driving laser with controllable CEP.

For Scenario #1 we find that at pulse energies so as to create few-MeV level electrons (Fourier-limited powers of 80, 90, 100 TW), the addition of PFC has a significant effect on the maximum electron energy after interaction, and the addition of small amounts of chirp can optimise the energy further. This is summarized in Fig. 2. The acceleration decreases for all GDD values when the PFC is zero, matching previous results [23], showing that the effect can only be optimized with non-zero PFC. Note that for the three power levels studied the magnitude of optimum PFC increases, along with the optimum GDD, and also the relative improvement when adding PFC. The optimum PFC is always negative, but the optimum GDD at a given amount of PFC always has the same sign as that PFC.

For Scenario #2 we use also laser energies to generate few-MeV level electrons, but in this case it requires significantly less power (Fourier-limited powers of 5, 7, 9 TW) since the electrons have an initial non-zero energy and start immediately at an advantageous phase. Of course, to drive the relativistic plasma-mirror process that this scenario is meant to emulate, requires relativistic intensities and therefore higher laser powers. The sub-unity reflectivity of the plasma-mirror and degradation of any other relevant properties would result in a lower effective power taking part in the vacuum laser acceleration after reflection. These complex dynamics aren't taken in to account, so this must be taken in context when interpreting the results.

The addition of PFC in this scenario also has an effect on the maximum electron energy after interaction, seen in Fig. 3, with the effect and the optimum amount of PFC increasing with the energy of the driving laser as

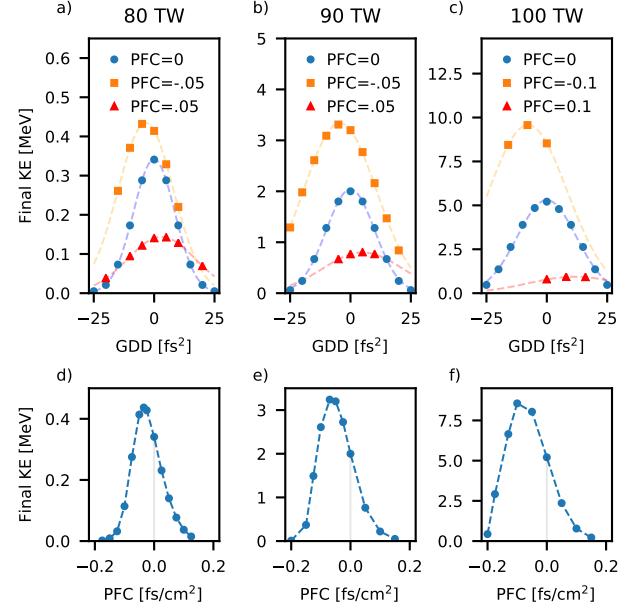


FIG. 2. Results from Scenario #1 with Fourier-limited powers of (a,d) 80, (b,e) 90, and (c,f) 100 TW. The top row (a–c) is final kinetic energies for many combinations of PFC and chirp with the dashed lines Gaussian fits, and the bottom row (d–f) is for zero chirp and various amounts of PFC with the dashed lines as guides for the eyes. PFC is in units of fs/cm² always.

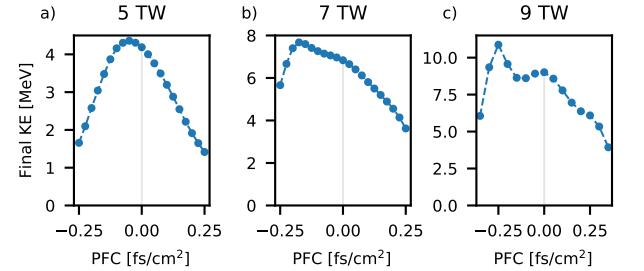


FIG. 3. Results for varying levels of PFC in Scenario #2 with Fourier-limited powers of (a) 5, (b) 7, and (c) 9 TW.

seen before. The effect is however smaller relative to the accelerated energies present, producing only an increase of 21 % in the case of 9 TW driving power. This is likely due to the fact that the electron begins with non-zero energy, so the advantageous situation does not act as effectively.

In both scenarios the optimum PFC value is negative, with all positive values of PFC producing lower net acceleration. The striking result of an increased final kinetic energy with this imparted spatio-temporal coupling (and therefore a slightly lower peak intensity) provides direct motivation for the opportunity to optimize the acceleration process via specific fine-tuning of the PFC. However,

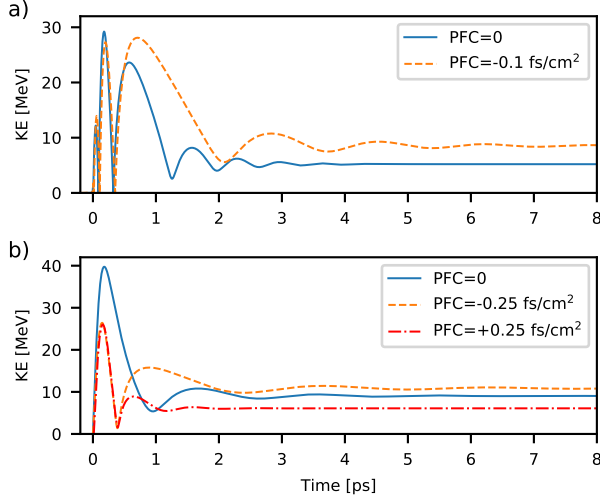


FIG. 4. Comparison of trajectories from (a) Scenario #1 with 100 TW and (b) Scenario #2 with 9 TW. Shown are the default case (PFC=GDD=0) (solid), the improved case (dashed), and a worsened case (dot-dashed).

this decrease at positive values of PFC provides a useful insight into experiments as well. If there is an undiagnosed level of PFC, then the acceleration process could be either enhanced or damped. For example, in the case of acceleration with a Fourier-limited 90 TW beam a PFC of $+0.05 \text{ fs/cm}^2$ results in a decrease in final kinetic energy by a factor of 2.6 (without any chirp). However, on a beam of $w_i=4 \text{ cm}$ with $f=0.63 \text{ m}$ this level of PFC causes a decrease in peak intensity of only 2.5 % and is equivalent to a delay of only 0.8 fs at the edge of the beam. Therefore, detailed knowledge of spatio-temporal couplings or the lack thereof — possible with developing full spatio-temporal characterization devices [24, 25], or with diagnostics made specifically for measuring PFC [26, 27] — is crucial to not only optimizing the mechanism, but having it perform at a nominal level.

We can also compare the trajectories of representative simulations in each scenario in an attempt to understand the mechanism, seen in Fig. 4. In both scenarios the optimized case with PFC shows the same general behavior relative to the case without PFC. With negative PFC the peak energy reached during the peak accelerating cycle is lower, but in subsequent laser cycles the electron is decelerated less, and accelerated more, leading to a higher final energy. This is sensible, since the peak field is lower in this main accelerating cycle, but the PFC has provided an advantageous situation for the region outside of the intensity peak. Since PFC removes the time symmetry of the pulse in focus, this also provides an insight in to why the final kinetic energy is lower with positive PFC. In the case of positive PFC the peak kinetic energy is also lower, but the following cycles have a disadvantageous situation and the final kinetic energy is still lower than

the default case. This is seen most clearly in comparing the dot-dashed trajectory to the dashed trajectory in the bottom panel of Fig. 4.

The results in other focusing conditions, with shorter pulse durations, larger driving laser power, or different central frequency are beyond the scope of this work. However, preliminary simulations show that the effect of PFC on focused intensity is larger as the pulse duration is decreased, the trade-off between improved accelerating phase and decreased intensity is less able to result in an increased final kinetic energy. So it may be that the PFC is only a detrimental quantity for other driving laser parameters. Scaling with wavelength is discussed in the literature [3], and the effect of spatio-temporal distortions in developing THz sources is also of potential interest. At higher laser powers, shorter durations, or tighter focusing, non-paraxial terms and a sech^2 temporal profile would need to be used for satisfactory accuracy.

Experimentally, it is possible to compensate for an existing level of PFC [28], but such compensation or tuning mechanisms are not common-place or simple. Additionally, PFC can come from many sources in ultrafast laser systems so it is difficult to remove completely from the final high-power beam without taking great care. Therefore, practically, the results of these studies do provide an avenue for optimization, but the more relevant result may be that the amount of PFC necessary to spoil the mechanism is very small.

The results in summary mean that the specifically applied spatio-temporal coupling of PFC (or longitudinal chromatism) can increase the final kinetic energy of a single electron accelerated on-axis by a focused ultrashort radially-polarized laser beam. This can be increased further with the addition of small amounts of linear chirp. In the general case of Scenario #1, where the initial particle position and the laser CEP are freely varied, this results in almost doubling the energy when accelerated with a 100 TW beam. In the more restricted case of Scenario #2, meant to emulate the case of the laser interacting with a relativistic plasma mirror surface, there is also limited improvement with the addition of PFC. In both scenarios simulated there is a drastic decrease of the final kinetic energy at PFC values of positive sign, opposite that of the optimum, motivating the characterization of spatio-temporal couplings in any experiment of this kind. Beyond the impact on on-axis vacuum laser acceleration presented here, specific combinations of other low- or high-order spatial-temporal couplings may prove useful in particle manipulation or engineering specific laser-material interaction.

Funding. The work was supported by the fellowship CEA-Eurotalents.2014-2018 (n° PCOFUND-GA-2013-600382) under the Seventh Framework Program (FP7).

Acknowledgement. The author would like to thank Raphaël Lebrun, Antoine Jeandet, and Fabien Quéré for helpful discussions and comments.

* spencer.jolly@cea.fr

- [1] Y. I. Salamin, Optics Letters **31**, 2619 (2006).
- [2] Y. I. Salamin, Optics Letters **32**, 90 (2007).
- [3] L. J. Wong and F. X. Kärtner, Optics Express **18**, 25035 (2010).
- [4] V. Marceau, A. April, and M. Piché, Optics Letters **37**, 2442 (2012).
- [5] V. Marceau, C. Varin, T. Brabec, and M. Piché, Physical Review Letters **111**, 224801 (2013).
- [6] A. Sell and F. X. Kärtner, Journal of Physics B: Atomic, Molecular and Optical Physics **47**, 015601 (2014).
- [7] C. Varin, V. Marceau, P. Hogan-Lamarre, T. Fennel, M. Piché, and T. Brabec, Journal of Physics B: Atomic, Molecular and Optical Physics **49**, 024001 (2016).
- [8] L. J. Wong, K.-H. Hong, S. Carbajo, A. Fallahi, P. Piot, M. Soljačić, J. Joannopoulos, F. X. Kärtner, and I. Kaminer, Scientific Reports **7**, 11159 (2017).
- [9] S. Payeur, S. Fourmaux, B. E. Schmidt, J. P. MacLean, C. Tchervakov, F. Légaré, M. Piché, and J. C. Kieffer, Applied Physics Letters **101**, 041105 (2012).
- [10] S. Carbajo, E. A. Nanni, L. J. Wong, G. Moriena, P. D. Keathley, G. Laurent, R. J. D. Miller, and F. X. Kärtner, Physical Review Accelerators and Beams **19**, 021303 (2016).
- [11] P.-L. Fortin, M. Piché, and C. Varin, Journal of Physics B: Atomic, Molecular and Optical Physics **43**, 025401 (2010).
- [12] C. Thauray, F. Quéré, J.-P. Geindre, A. Levy, T. Ceccotti, P. Monot, M. Bougeard, F. Réau, P. D'Oliveira, P. Audebert, R. Marjoribanks, and P. Martin, Nature Physics **3**, 424 (2007).
- [13] M. Thévenet, A. Leblanc, S. Kahaly, H. Vincenti, A. Vernier, F. Quéré, and J. Faure, Nature Physics **12**, 355 (2016).
- [14] N. Zaim, M. Thévenet, A. Lifschitz, and J. Faure, Physical Review Letters **119**, 094801 (2017).
- [15] M. Thévenet, H. Vincenti, and J. Faure, Physics of Plasmas **23**, 063119 (2016).
- [16] L. J. Wong and F. X. Kärtner, Optics Letters **36**, 957 (2011).
- [17] S. Akturk, X. Gu, P. Bowlan, and R. Trebino, Journal of Optics **12**, 093001 (2010).
- [18] Z. Bor, Optics Letters **14**, 119 (1989).
- [19] A. Sainte-Marie, O. Gobert, and F. Quéré, Optica **4**, 1298 (2017).
- [20] D. H. Froula, D. Turnbull, A. S. Davies, T. J. Kessler, D. Haberberger, J. P. Palastro, S.-W. Bahk, I. A. Begishev, R. Boni, S. Bucht, J. Katz, and J. L. Shaw, Nature Photonics (2018), 10.1038/s41566-018-0121-8.
- [21] W. Holgado, C. Hernández-García, B. Alonso, M. Miranda, F. Silva, O. Varela, J. Hernández-Toro, L. Plaja, H. Crespo, and I. J. Sola, Physical Review A **95**, 063823 (2017).
- [22] V. Marceau, C. Varin, and M. Piché, Optics Letters **38**, 821 (2013).
- [23] P. Hogan-Lamarre, V. Marceau, C. Varin, T. Brabec, and M. Piché, *2015 European Conference on Lasers and Electro-Optics - European Quantum Electronics Conference*, 2015 European Conference on Lasers and Electro-Optics - European Quantum Electronics Conference , CG_P.19 (2015).
- [24] G. Pariente, V. Gallet, A. Borot, O. Gobert, and F. Quéré, Nature Photonics **10**, 547 (2016).
- [25] A. Borot and F. Quéré, Optics Express **26**, 26444 (2018).
- [26] Z. Bor, Z. Gogolak, and G. Szabo, Optics Letters **14**, 862 (1989).
- [27] Z. Li, N. Miyanaga, and J. Kawanaka, Optics Letters **43**, 3156 (2018).
- [28] S.-W. Bahk, J. Bromage, and J. D. Zuegel, Optics Letters **39**, 1081 (2014).